EVS27
Barcelona, Spain, November 17-20, 2013

Design and Evaluation of a Wireless Power Transfer System with Road Embedded Transmitter Coils for Dynamic Charging of Electric Vehicles

Kraisorn Throngnumchai[1], Akihiro Hanamura[1], Yuji Naruse[1], Kazuhiro Takeda[2]
[1]*EV System Lab., Nissan Research Center, Nissan Motor co., ltd., 1-1, Morinosatoaoyama, Atsugi-shi, Kanagawa 243-0123, JAPAN*
t-kraisorn@mail.nissan.co.jp
[2] *Research Testing Section No.1, Nissan Research Center, Nissan Motor co., ltd., 1-1, Morinosatoaoyama, Atsugi-shi, Kanagawa 243-0123, JAPAN*

Abstract

The cruising range of an electric vehicle (EV) can be greatly extended by a dynamic wireless charging system because the battery can be charged while the vehicle is moving. However, the investment in infrastructure can be enormous and has to be reduced to implement the system. This paper presents the design of a wireless power transfer system with road embedded transmitter coils to facilitate dynamic charging of EVs. A 30 cm by 1.6 m transmitter coil, which is relatively long compared with the 40-cm-diameter circular receiver coil, has been designed to reduce the cost of the transmitter circuit. A prototype transmitter coil has been embedded into a road for evaluation of its characteristics. The measured coupling coefficient of the transmitter and receiver coils is as small as 0.09 because of the asymmetry between the coils. Compensation circuits for the transmitter and receiver coils have been designed and optimized for such a small coupling coefficient condition. The designed dynamic charging system can transfer more than 1 kW of electric power with more than 90% efficiency. Five transmitter circuits have been embedded into a road surface for testing. Cement asphalt mortar was used to construct the road surface in this study to avoid damaging the transmitter coils by high temperature and high pressure during the construction work. The designed receiver circuit has been installed on a compact 2-seater EV. A demonstration was conducted to show that the retrofitted EV can successfully receive electric power transferred from the road.

Keywords: electric vehicle, dynamic charging, wireless power transfer, coil, compensation circuit

1 Introduction

Electric vehicles (EVs) are expected to be a key technology in improving energy sustainability for tomorrow's personal mobility because electricity can be generated from various power sources, including renewable energies such as solar, wind, geothermal, and so on. However, the cruising range of EVs is currently limited due to the necessity of recharging their batteries periodically. Improving the battery's power density and adopting advanced technologies such as plug-in hybrids and fuel cell vehicles are among the approaches proposed for extending the cruising

range [1-4]. Among these technologies, a wireless dynamic charging system can charge EV batteries while the vehicles are moving and thereby greatly extend their cruising range [5]. There will be no need to go to a charging station and EV users will not experience any range anxiety wherever such infrastructure is available. The following are some of the advantages of dynamic charging.

1. Improves the effectiveness of space and time necessary for charging because the battery is recharged on the road during a trip.
2. Eliminates the range anxiety associated with EVs.
3. Avoids queuing at charging stations.
4. Enables unrestricted cruising where the infrastructure is available.
5. Minimizes the size and cost of the on-board battery pack.

A drawback of a dynamic charging system is the necessary infrastructure. The in-road power transmitter system must be carefully designed to obtain sufficient power transfer efficiency and performance. Moreover, the investment in infrastructure for dynamic charging can be very large. Reducing the cost of constructing the infrastructure is necessary to promote practical use of such a system.

This paper presents the design and evaluation of a dynamic charging system. Firstly, the design of the transmitter and receiver coils is explained in section 2. The transmitter coil of the designed system is relatively long compared with the receiver coil in order to reduce the transmitter circuit cost. This asymmetry results in a small coupling coefficient between the transmitter and receiver coils. Estimations of the self and mutual inductance of both the transmitter and receiver coils are presented and compared with the measured results.

The compensation circuits designed for both the transmitter and the receiver are discussed in section 3. These compensation circuits have been designed and optimized to enable power transfer under a small coupling coefficient condition. The designed system has the capability to transfer more than 1 kW of electric power. Simulation results are presented together with the results measured on a test bench.

The designed transmitter coil has been embedded into a test road for evaluation of its characteristics. A suitable construction method and materials were selected for the test road to avoid damaging the buried transmitter coil. The road construction method and materials used in this study are described in section 4.

The designed receiver coil has been implemented on a compact 2-seater EV. A demonstration that was conducted to show that the retrofitted EV can receive electric power from the road is also explained in section 4. Lastly, the final section presents the conclusions and plans for future work.

2 Coils and Their Characteristics

A relatively long transmitter coil as compared with the receiver coil was used in this study to reduce the cost of the infrastructure necessary for the dynamic charging system. This asymmetry reduces the coupling coefficient between the transmitter and receiver coils and decreases the transferable power of the system. Both the transmitter and receiver coils must be carefully designed with respect to self and mutual inductance in order to obtain sufficient transferable power.

In this section, the design of the transmitter coil is firstly explained and compared with the measured results, followed by an explanation of the design and measured results of the receiver coil.

2.1 Transmitter Coil

A 30 cm by 1.6 m, 3-turn, rectangular coil has been designed for the transmitter. Figure 1 shows a schematic of the transmitter coil used in this study.

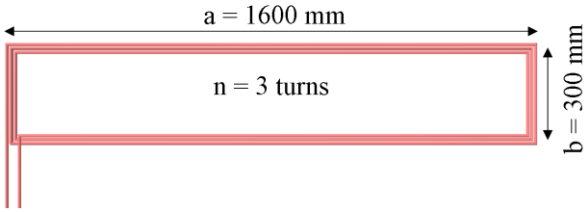

Figure1: Schematic of the transmitter coil used in this study

The inductance L of a rectangular coil can be estimated with the following equation.

$$L = \frac{\mu_0 \cdot n^2}{\pi} \cdot \left(b \cdot \ln \frac{a}{r} + a \cdot \ln \frac{b}{r} \right) \quad (1)$$

where a, b, r, n stand for the length, width, and radius of the wire used to construct the coil, and the number of turns of the coil, respectively.

Parameter a is 1.6 m for the transmitter coil shown in Fig. 1, b is 0.3 m and n is 3. The Litz wire used to build the coils examined in this study has a radius r of 3 mm and can carry electric current up to 40 A_{rms}. The inductance of the transmitter coil used in this study was estimated from Eq. (1) to be 33 uH.

The inductance and quality factor (Q-factor) of the transmitter coil were measured in a shielded room as a function of frequency using an LCR meter. Figure 2 shows a photograph of the measured transmitter coil.

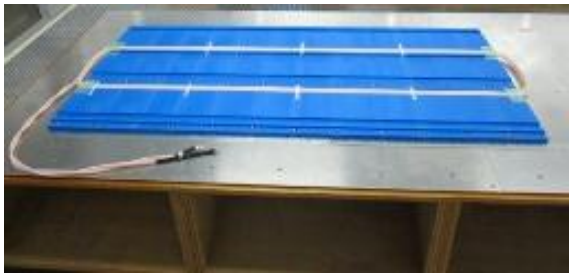

Figure2: Photograph of the measured transmitter coil

Figure 3 shows the measured inductance and Q-factor of the transmitter coil as a function of frequency. The solid blue line in the figure indicates the inductance and the dashed red line is the Q-factor.

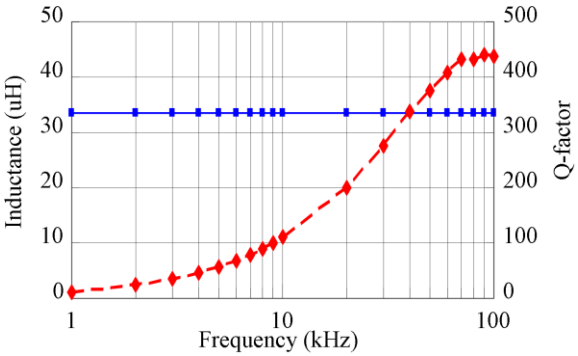

Figure3: Measured inductance and Q-factor of the transmitter coil as a function of frequency. The solid blue line shows the inductance and the dashed red line the Q-factor.

It is seen in Fig. 3 that the value of the measured inductance of the transmitter coil was 33 uH, which agrees well with the inductance estimated using Eq. (1). It is also seen that the measured Q-factor of the transmitter coil reached its peak of 440 at a frequency of 90 kHz.

2.2 Receiver Coil

A 40-cm-diameter, 6-turn, circular coil has been designed for the receiver. Figure 4 shows a schematic of the receiver coil used in this study.

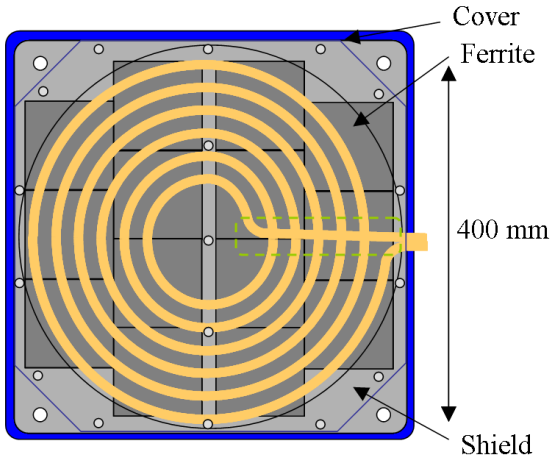

Figure4: Schematic of the receiver coil used in this study

Ferrite and aluminium are used to shield and protect the body of the test vehicle from being exposed to the magnetic field emitted from the transmitter coil when the receiver coil is installed on an EV.

The inductance L of a circular coil can be estimated with the following equation.

$$L = \mu_0 \cdot R \cdot n^2 \cdot \left(\ln \frac{8R}{r} - 2 \right) \qquad (2)$$

where R stands for the average radius of the coil. Parameters r and n have the same meaning as in Eq. (1).

The inductance of the receiver coil used in this study was estimated from Eq. (2) to be 27 uH, assuming an average coil radius R of 150 mm and the same wire radius r as that of the transmitter coil. The inductance and Q-factor of the receiver coil were measured as a function of frequency in the same manner as for the transmitter coil. Figure 5 shows a photograph of the measured receiver coil.

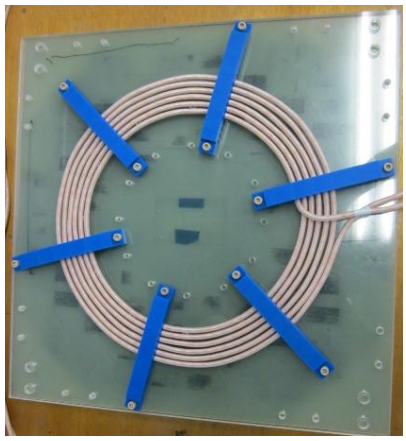

Figure5: Photograph of the measured receiver coil

Figure 6 shows the measured inductance and Q-factor of the receiver coil as a function of frequency. The solid blue line in the figure is the inductance and the dashed red line is the Q-factor.

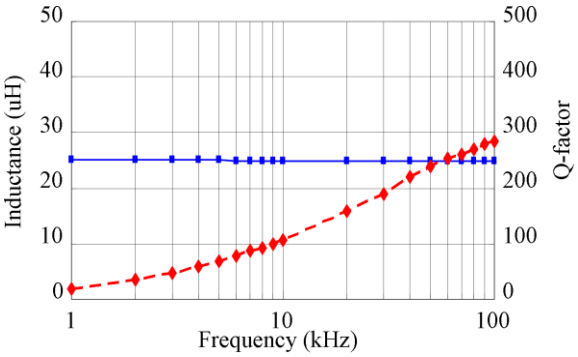

Figure6: Measured inductance and Q-factor of the receiver coil as a function of frequency. The solid blue line shows the inductance and the dashed red line the Q-factor.

It is seen in Fig. 6 that the value of the measured inductance of the receiver coil was 27 uH, which coincides well with the inductance estimated using Eq. (2) when the average radius R was assumed to be 150 mm. It is also seen in the figure that the maximum value of the measured Q-factor of the receiver coil was 280 at a frequency of 100 kHz.

2.3 Coupling Coefficient between the Transmitter and Receiver Coils

When the receiver coil is positioned above the transmitter coil at a height h as shown in Fig. 7, the coupling coefficient κ between the coils is proportional to the ratio of the overlapped area of the coils to the area of the transmitter coil and inversely proportional to the third power of the distance between the coils. In this study where b < 2R, κ can be estimated with the following equation.

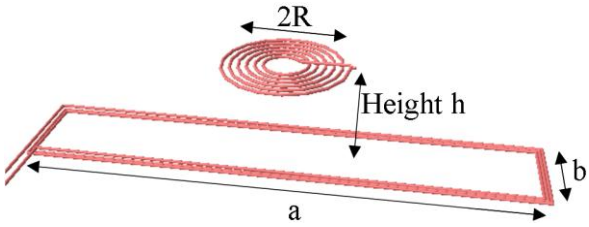

Figure7: Schematic showing the receiver coil positioned above the transmitter coil

$$\kappa = \frac{2R}{a} \cdot \left(\frac{R}{\sqrt{b^2 + 4h^2}} \right)^3 \qquad (3)$$

Figure 8 shows the measured coupling coefficient as a function of h compared with the value estimated using Eq. (3).

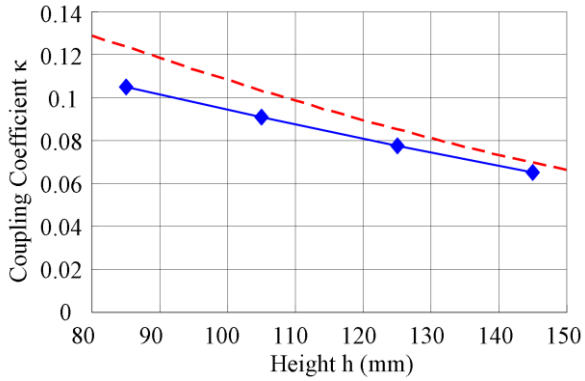

Figure8: Coupling coefficient κ as a function of height h. The solid blue line shows the measured value and the dashed red line the value estimated with Eq. (3).

As seen in Fig. 8, the measured values agree well with the estimation. The coupling coefficient κ was found to be 0.09 when the height h was 100 mm.

The cost per unit distance of the infrastructure can be reduced by using a longer transmitter coil because less power electronic equipment and fewer compensation circuits are required for the same road length. However, it can be found from Eq. (3) that the coupling coefficient κ decreases with a longer transmitter coil, i.e., larger a. A smaller κ results in lower power transfer efficiency η and also smaller transferable power of the system.

Theoretically, the maximum power transfer efficiency η of the system can be calculated by analysing the circuit shown in Fig. 9 as follows.

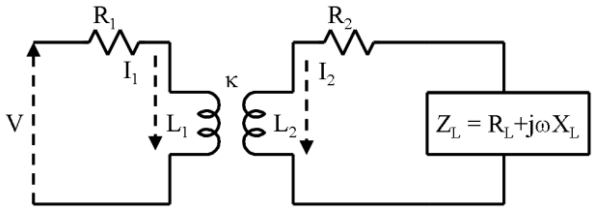

Figure9: Schematic circuit diagram used to analyze the theoretical maximum power transfer efficiency η

$$\eta = \frac{I_2^2 R_L}{I_1^2 R_1 + I_2^2 R_2 + I_2^2 R_L} = \frac{R_L}{\frac{(R_2 + R_L)^2 + (\omega L_2 + X_L)^2}{(\omega M)^2} R_1 + R_2 + R_L} \quad (4)$$

$$\therefore \eta_{\max} = \frac{1}{1 + \frac{2}{\kappa^2 Q_1 Q_2} + 2\frac{\sqrt{\kappa^2 Q_1 Q_2 + 1}}{\kappa^2 Q_1 Q_2}} \quad (5)$$

The theoretical maximum power transfer efficiency η_{max} shown in Eq. (5) can be obtained only by applying a proper load given by the following equation.

$$R_{L\max} = R_2\sqrt{1 + \kappa^2 Q_1 Q_2} \quad (6)$$

$$X_{L\max} = -\omega L_2 \quad (7)$$

When the height h of the receiver coil from the transmitter coil is 100 mm and the operating frequency is 90 kHz, κ equals 0.09, Q_1 440, and Q_2 280, respectively. The maximum power transfer efficiency η_{max} of the designed system was calculated with Eq. (5) to be 94%.

In actuality, because a proper load cannot be selected, it is difficult to obtain the maximum power transfer efficiency η_{max}. Compensation circuits for the transmitter and the receiver must be carefully designed to prevent any further fall in power transfer efficiency η. The design of the compensation circuits will be described in the next section.

3 Compensation circuits

A compensation circuit with two resonators as described in Ref. [6] is better suited for optimizing the system under a small coupling coefficient condition because it allows greater freedom for selecting the resonant frequency of the additional resonator. This type of compensation circuit was designed for both the transmitter and the receiver in this study. The simulation and measured characteristics of the designed circuit are described here.

Figure 10 shows a schematic diagram of the designed circuit.

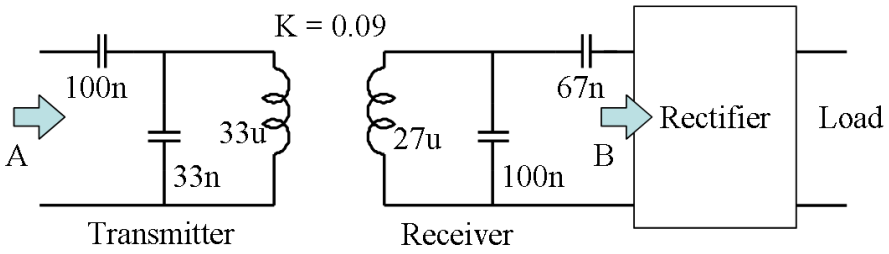

Figure10: Schematic circuit diagram of the designed transmitter and receiver circuits used in this study

A rectifier with a 12-Ω resistor is used as the load of the circuit shown in Fig. 10. Figure 11 shows the simulated input voltage and current at point A in Fig. 10, and Fig. 12 shows the simulated output voltage and current at point B in Fig. 10. A frequency of 78 kHz was used in the simulation.

The solid blue line in both figures shows the current and the dashed red line the voltage.

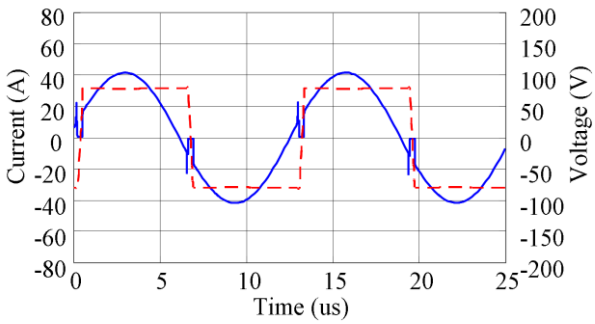

Figure11: Simulated voltage and current at point A in Fig. 10. The solid blue line shows the current and the dashed red line the voltage.

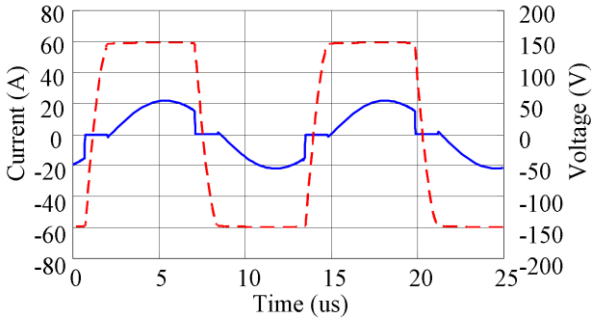

Figure12: Simulated voltage and current at point B in Fig. 10. The solid blue line shows the current and the dashed red line the voltage.

The phase difference θ between the voltage and current at points A and B can be found from Figs. 11 and 12 to be about 20°, and the power factor cos θ at both points is about 0.94. This power factor level is sufficiently high for power to be transferred at sufficiently high efficiency.

The voltage, current and power were measured using a shielded test bench. Figures 13, 14, 15 and 16 compare the simulated and measured results.

The voltage and current of the transmitter coil are shown in Figs. 13 and 14, respectively. The solid blue line in both Fig. shows the measured results and the dashed red line the simulated result.

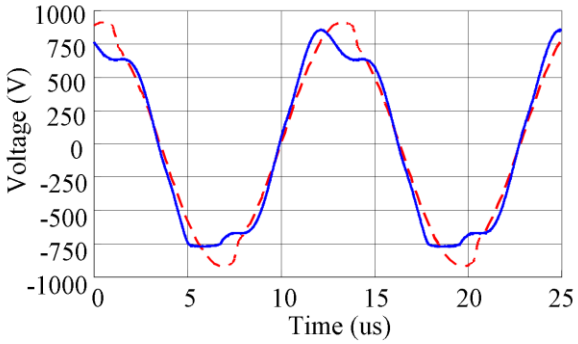

Figure13: Simulated and measured voltage of the transmitter coil. The solid blue line shows the measured result and the dashed red dash line the simulated result.

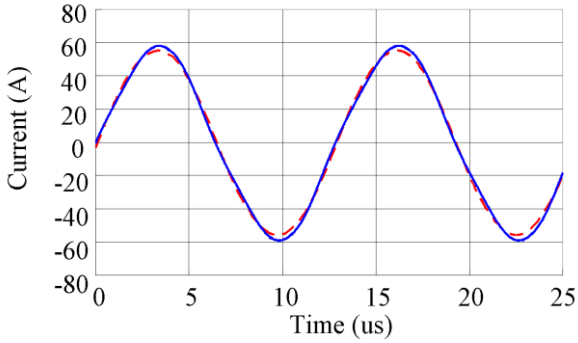

Figure14: Simulated and measured current of the transmitter coil. The solid blue line shows the measured result and the dashed red dash line the simulated result.

It is seen in Figs. 13 and 14 that both the measured voltage and current of the transmitter coil agree very well with the simulation results. It is also seen in Fig. 14 that the current flowing in the transmitter coil is smaller than 40 $A_{rms,}$ which is the maximum limit that the Litz wire used in this study can carry.

The voltage and current of the receiver coil are shown in Figs. 15 and 16, respectively.

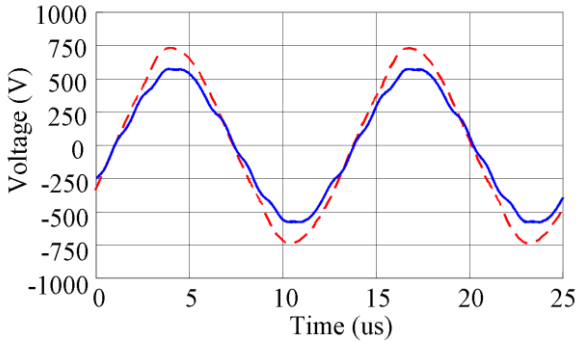

Figure15: Simulated and measured voltage of the receiver coil. The solid blue line shows the measured result and the dashed red line the simulated result.

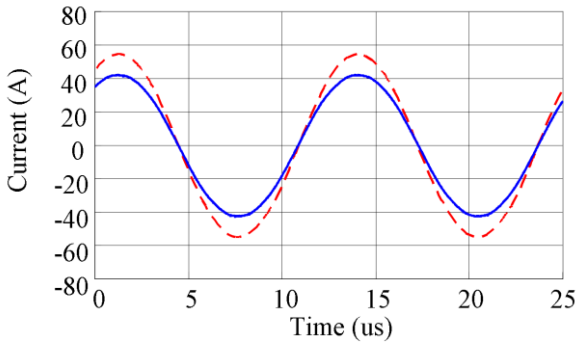

Figure16: Simulated and measured current of the receiver coil. The solid blue line shows the measured result and the dashed red dash line the simulated result.

Again, it is seen in Figs. 15 and 16 that both the measured voltage and current agree well with the corresponding simulation results.
The power transferred to the load by the designed system was measured using a power meter to be 1.176 kW.
The power transfer efficiency η was measured to be 92.8%. The difference between the measured η and ηmax calculated from Eq. (5) is attributed to the distortion observed in the waveforms shown in Figs. 15 and 16.

4 Test Road Construction

Five transmitter circuits were embedded in a road surface to build a 10-m-long test road. To demonstrate that an EV can dynamically receive electric power from the road, the receiver circuit was installed on a compact 2-seater EV and tested.
This section first explains the road construction method and materials used and then describes the retrofitted EV together with the demonstration results.

4.1 Construction Methodology

Usually, hot mix asphalt concrete is used to construct the road surface. In this type of construction, the asphalt binder has to be heated to about 150 °C (300 °F) to reduce its viscosity prior to the mixing process. In order to obtain sufficiently dense concrete, it is usually compacted under pressure after the paving process while the asphalt is sufficiently hot.
In this study Litz wire was used for both the transmitter and receiver coils. Litz wire consists of multiple thin wire strands insulated electrically from each other. This structure reduces the skin effect and proximity effect losses, and increases the Q-factor of the coils as a result. However, because of its structure, Litz wire cannot withstand exposure to high temperature and mechanical stress. Therefore, hot mix asphalt concrete was not a suitable material for constructing the test roadway because the paving and compaction processes might damage the transmitter coil.
Accordingly, a cement asphalt mortar (CAM) was selected for constructing the test road surface. CAM is produced by emulsifying asphalt in water with soap. It can be used for paving at room temperature. Moreover, the ratio of emulsified asphalt, cement and silica sand of the CAM used in this study was selected to be 1.4:1:1 because this ratio provides sufficient density without requiring compaction.
The first step of the road construction process was to cut the road surface to a depth of 50 mm.
Figures 13 and 14 show a photograph of the transmitter coil embedded in the test road and the road paving process.

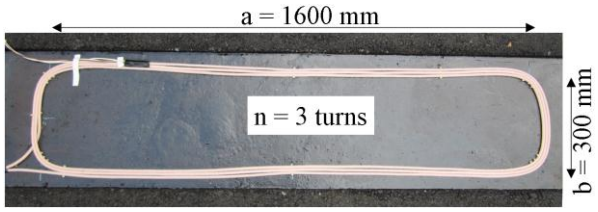

Figure13: Photograph of the transmitter coil embedded in the test road

Figure14: Photograph showing the paving of the test road

Figure 15 shows a schematic cross-sectional view of the constructed test road. The transmitter coils were embedded at a depth of 30 mm from the road surface.

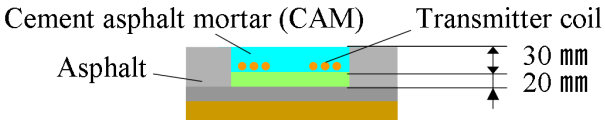

Figure15: Schematic cross-sectional view of the test road

Figure 16 shows a photograph of the constructed test road after paving and lane mark painting.

Figure16: Photograph of the constructed test road after paving and lane mark painting

The inductance and Q-factor of the embedded transmitter coils were measured after the construction work. No changes were found in either the inductance or the Q-factor of the coils compared with the corresponding values measured before the construction work. This indicated that damage to the transmitter coils during the construction work was prevented by the materials and construction process used.

4.2 EV for demonstration

The designed receiver circuit was implemented on a compact 2-seater EV called the Nissan New Mobility Concept to demonstrate that electric power can be transferred from the road while the EV is moving. A photograph of the retrofitted EV is shown in Fig. 17.

Figure17: Photograph of the EV used in the demonstration

Figure 18 shows a photograph of the receiver coil installed at the rear of the test EV.

Figure18: Photograph of the receiver coil installed at the rear of the test EV

LED panels were installed to indicate that the EV received electric power from the road.

The electric power for the demonstration was controlled to be less than 50 W to meet the radio wave limit in Japan.

Figure 19 shows a photograph of an LED panel while the EV was running on the test road. It is seen in the figure that the LED panel was illuminated, which indicated that the EV successfully received electric power from the road.

Figure19: Photograph of an LED panel while the EV was running on the test road

5 Conclusions and Future Works

This paper has presented the design and evaluation of a wireless power transfer system with road embedded transmitter coils for dynamic charging of an EV. While the radius of the circular receiver coil was designed to be 0.2 m, the transmitter coil was designed with a relatively long length of 1.6 m. This asymmetry reduces the coupling coefficient κ between the coils. Compensation circuits for both the transmitter and the receiver were optimized for a small κ condition. A test bench measurement showed that the designed system can transfer more than 1 kW of electric power with more than 90% efficiency.

Five transmitter circuits were embedded in a test road surface. Cement asphalt mortar (CAM) was selected as the material for constructing the test road to avoid exposing the transmitter coils to high temperature and high pressure.

The receiver circuit was implemented on a compact 2-seater EV. A demonstration showed that the test EV successfully received electric power from the road.

In future works it is planned to investigate the electromagnetic interference (EMI) emitted from the transmitter coils. Further reduction of EMI is necessary to increase the transferable power in actual use.

The system described in this paper has been designed and optimized only for unidirectional electric power transfer from the road to the vehicle. A study on bidirectional power flow between the infrastructure and the on-board battery, which is essential to facilitate a vehicle-to-grid (V2G) concept, is also planned for future work [7].

Acknowledgments

The authors would like to thank Dr. Nagato Abe, Michio Yoshitake, Kazunao Aoki, Hiroshi Nitta and Kazunori Manabe of Toa Road Corporation for their valuable discussions and support regarding the construction of the test road.

References

[1] N. Savage, *Batteries That Breathe, Using oxygen as a cathode could give lithium batteries 10 times the energy*, IEEE Spectrum, vol. 48, Feb. 2011, 13

[2] M. Doude and G. M. Molen, *Design Methodology for a Range-Extended PHEV*, IEEE VPPC 2009, Sep. 2009, 817-819

[3] H. B. Jensen et. al., *Evaluation of Fuel-Cell Range Extender Impact on Hybrid Electrical Vehicle Performance*, IEEE Trans. Vehicular Tech., vol. 62, No. 1, Jan. 2013, 50-60

[4] R. Eckl et. al., *Alternative Range Extender for Electric Cars – Zinc Air Batteries*, Conf. on Future Automotive Tech., 2013, 3-18

[5] S. Ahn et. al., *Charging up the road, If electric vehicles could draw power from the streets, there's no telling how far they could go*, IEEE Spectrum, vol. 50, Apr. 2013, 44-50

[6] K. Throngnumchai et. al., *A Study on Receiver Circuit Topology of a Cordless Battery Charger for Electric Vehicles*, IEEE ECCE 2011, 843-850

[7] D. J. Thrimawithana et. al., *Design of a Bi-Directional Inverter for a Wireless V2G System*, IEEE ICSET 2010, Dec. 2010, 1-5

Authors

Dr. Kraisorn Throngnumchai was born in Bangkok, Thailand in 1958. He received his Bachelor's, Master's, and Ph.D. degrees in semiconductor devices from the University of Tokyo in 1981, 1983, and 1986, respectively. He is a Japanese licensed professional engineer. In 1986, he joined the Nissan Research Center of Nissan Motor Co., Ltd. where he is now a research manager in the EV Systems Laboratory. His current research interests include power electronics, image sensors, high-frequency circuitry, THz devices, automotive EMC, and wireless power transfer.

Akihiro Hanamura received his Bachelor's and Master's degrees from Touhoku University in 1989 and 1991, respectively. His current research interest is the circuit design of wireless power transfer systems.

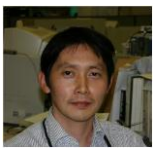

Yuji Naruse received his Bachelor's and Master's degrees from Kyoto University in 1996 and 1998, respectively. His current research interest is the magnetic design of wireless power transfer systems.

Kazuhiro Takeda joined Nissan Motor Co., Ltd. in 1988. He graduated from the Nissan technical college in 1994. His current research concern is on an automatic operation system.